Human alveolar macrophage response to *Mycobacterium tuberculosis*: immune characteristics underlying large inter-individual variability

[1,6,*]Wolfgang Sadee, [2,6]Ian H. Cheeseman, [1]Audrey Papp, [3]Maciej Pietrzak, [4]Michal Seweryn, [5]Xiaofei Zhou, [3]Shili Lin, [1]Amanda M. Williams, [2]Eusondia Arnett, [2]Abul K. Azad, and [2,*]Larry S. Schlesinger

[1]Center for Pharmacogenomics, Department of Cancer Biology and Genetics, College of Medicine, The Ohio State University. Columbus OH 43210

[2]Texas Biomedical Research Institute, 8715 W. Military Drive, San Antonio, TX 78227

[3]Department of Biomedical Informatics, College of Medicine, The Ohio State University. Columbus OH 43210

[4]Biobank Lab, Department of Molecular Biophysics, Faculty of Biology and Environmental Protection, University of Łódź, Łódź, Poland

[5]Department of Statistics, College of Arts and Sciences, The Ohio State University. Columbus OH 43210.

[6]These authors contributed equally to the work

[*]Corresponding authors (lschlesinger@txbiomed.org; wolfgang.sadee@osumc.edu)

Keywords: Tuberculosis, Alveolar Macrophages, Genomics, Systems Biology

Abstract

Mycobacterium tuberculosis (*M.tb)* establishes residence and growth in human alveolar macrophages (AMs). Large inter-individual variation in *M.tb*-AM interactions is a potential early indicator of TB risk and efficacy of therapies and vaccines. Herein, we systematically analyze interactions of a virulent *M.tb* strain with freshly isolated human AMs from 28 healthy adult donors, measuring host RNA expression and secreted candidate proteins associated with TB pathogenesis over 72h. We observe large inter-individual differences in bacterial uptake and growth, with tenfold variation in *M.tb* load at 72h, reflected by large variation of gene expression programs. Systems analysis of differential and variable RNA and protein expression identifies TB-associated genes and networks (*e.g.*, *IL1B* and *IDO1*). RNA time profiles document early stimulation of M1-type macrophage gene expression followed by emergence of an M2-type profile. The fine-scale resolution of this work enables the separation of genes and networks regulating early *M.tb* growth dynamics, and development of potential markers of individual susceptibility to *M.tb* infection and response to therapies.

Introduction

One-quarter of the world's population is approximated to be infected with *Mycobacterium tuberculosis* (*M.tb)*, and nearly 1.3 million people die annually from tuberculosis (TB), a continuing worldwide public health problem(WHO, 2020). While a substantial portion of the human population gets infected with *M.tb*, only a fraction of infected individuals progress to active TB. To control TB, we must understand the immunopathogenesis of *M.tb* infection, including host susceptibility or resistance

47 factors, to develop effective diagnostic, therapeutic and vaccine strategies for different
48 individuals and populations(Azad et al., 2020).

49 Aerosolized *M.tb* enters the lung alveolar space where it is phagocytosed by alveolar
50 macrophages (AMs), unique resident cells with a complex immunologic profile, to
51 become an intracellular pathogen. *M.tb* infection activates several macrophage
52 immunobiological pathways, including those involved in phagocytosis, phagosome-
53 lysosome trafficking, and triggering of inflammatory cytokines, oxidants, and cell
54 death pathways – all processes of innate immunity. Yet, critical factors that dictate
55 *M.tb* infection and progression to TB remain uncertain - a roadblock to understanding
56 an individual's susceptibility to TB(Guirado et al., 2013, Rajaram et al., 2014, Schorey
57 and Schlesinger, 2016).

58 The host response to *M.tb* infection ranges from complete clearance of infection to
59 latent infection to active TB(Pai et al., 2016). Therapy and vaccine trials further
60 highlight response variability across populations(Azad et al., 2020, Finan et al., 2008)
61 with BCG vaccination trials attaining only 50% efficacy(Colditz et al., 1994).
62 Evolutionary adaptation of *M.tb* to the host is considered a main factor modulating
63 virulence, host response, and TB severity(Sousa et al., 2020, Liu et al., 2017). For
64 example, evasion of immune surveillance by suppression of IL1B was proposed to be
65 largely dictated by virulence of the *M.tb* strain(Sousa et al., 2020); however,
66 expression of differentially expressed (DE) genes during infection with a single *M.tb*
67 strain can vary >10-fold between individuals(Azad et al., 2013). Therefore, both
68 genetic(Azad et al., 2012) and environmental/epigenetic(Thuong et al., 2008, Barreiro

69 et al., 2012, Moores et al., 2017, Rajaram et al., 2011) host factors also play a role,
70 while being less well understood.

71 Heritability estimates of susceptibility to TB range from 80% (twin and population
72 studies) to 25-50% polygenic risk scores(Naranbhai, 2016); yet, GWAS-significant
73 genetic variants alone fail to account for most of the estimated heritability(Naranbhai,
74 2016, Uren et al., 2017). Both *in vitro* and *in vivo* transcriptome studies of *M.tb*-
75 infected macrophages and other immune cells reveal DE candidate genes(Lavalett et
76 al., 2017, Roy et al., 2018, Rothchild et al., 2019, Moreira-Teixeira et al., 2020),
77 resulting in gene networks (Rajaram et al., 2014, Barreiro et al., 2012, Blischak et al.,
78 2015, Wu et al., 2014, Bragina et al., 2016), including type I IFN-associated
79 signatures in active TB(Moreira-Teixeira et al., 2020). Similarly, protein studies invoke
80 factors associated with TB status, including indoleamine oxidase 1 (IDO1), a marker
81 of active TB(Adu-Gyamfi et al., 2017). Complexity of these interacting processes
82 confound predictions of individual TB risk.

83 Our study addresses a critical gap in the field, the poorly understood variation of host
84 innate immune responses between individuals during *M.tb* infection, by characterizing
85 immune response genes and pathways that differ between individuals during infection
86 of human AMs from healthy donors with a single virulent *M.tb* strain. We identify host
87 genes and functional networks with highly variable expression between AM donors
88 correlating with *M.tb* growth dynamics in AMs, some already recognized as potential
89 biomarkers of active TB(Adu-Gyamfi et al., 2017, Gautam et al., 2018, Zak et al.,
90 2016, Moreira-Teixeira et al., 2020, Sousa et al., 2020).
91

92 **Results**

93 **Heterogeneity in *M.tb* uptake, adaptation and growth in human AMs among**
94 **donors**

95 We infected human AMs from 28 adult healthy donors over 2h with a virulent *M.tb*
96 strain ($H_{37}R_v$) engineered to emit light (luminescence RLU values), and followed RLUs
97 over 72h (**Figure 1A,B**). After batch effect correction, large variations in RLU values
98 are detectable at each time point (**Figure 1B; Supplementary File 1**). RLUs correlate
99 with *M.tb* colony forming units (CFUs), jointly reflecting the number of intracellular
100 bacilli and microbial metabolic activity(Salunke et al., 2015), while early RLU levels at
101 2-24h post-infection largely reflect *M.tb* cellular uptake and early intracellular
102 adaptation. AMs with the highest and lowest RLUs display a nearly tenfold difference
103 at 72h. *M.tb* growth rates (24-72h post infection) are consistent with the expected
104 *M.tb* doubling time (here referred to as generation time, in minutes required for
105 doubling over 48-72h post infection), while varying 2-3 fold between donors. The
106 assays presented throughout were conducted at a multiplicity of infection (MOI) of 2:1
107 (*M.tb*/AM cells). Bacterial growth rates (24-72h) were similar using a MOI of 10:1
108 (**Supplementary File 1**). To identify proteins and genes that influence *M.tb*-AM
109 interactions, we focus on generation times (48-72h) in this study, since RLU levels
110 prior to 48h post infection reflect *M.tb* uptake, adaptation, and early growth combined.

111 **Human AM-secreted proteins capture the immune response to *M.tb* infection**

112 To assess the inflammatory mediator response by macrophages to *M.tb* infection, we

113 measured 27 secreted proteins, previously implicated in cellular responses to *M.tb*

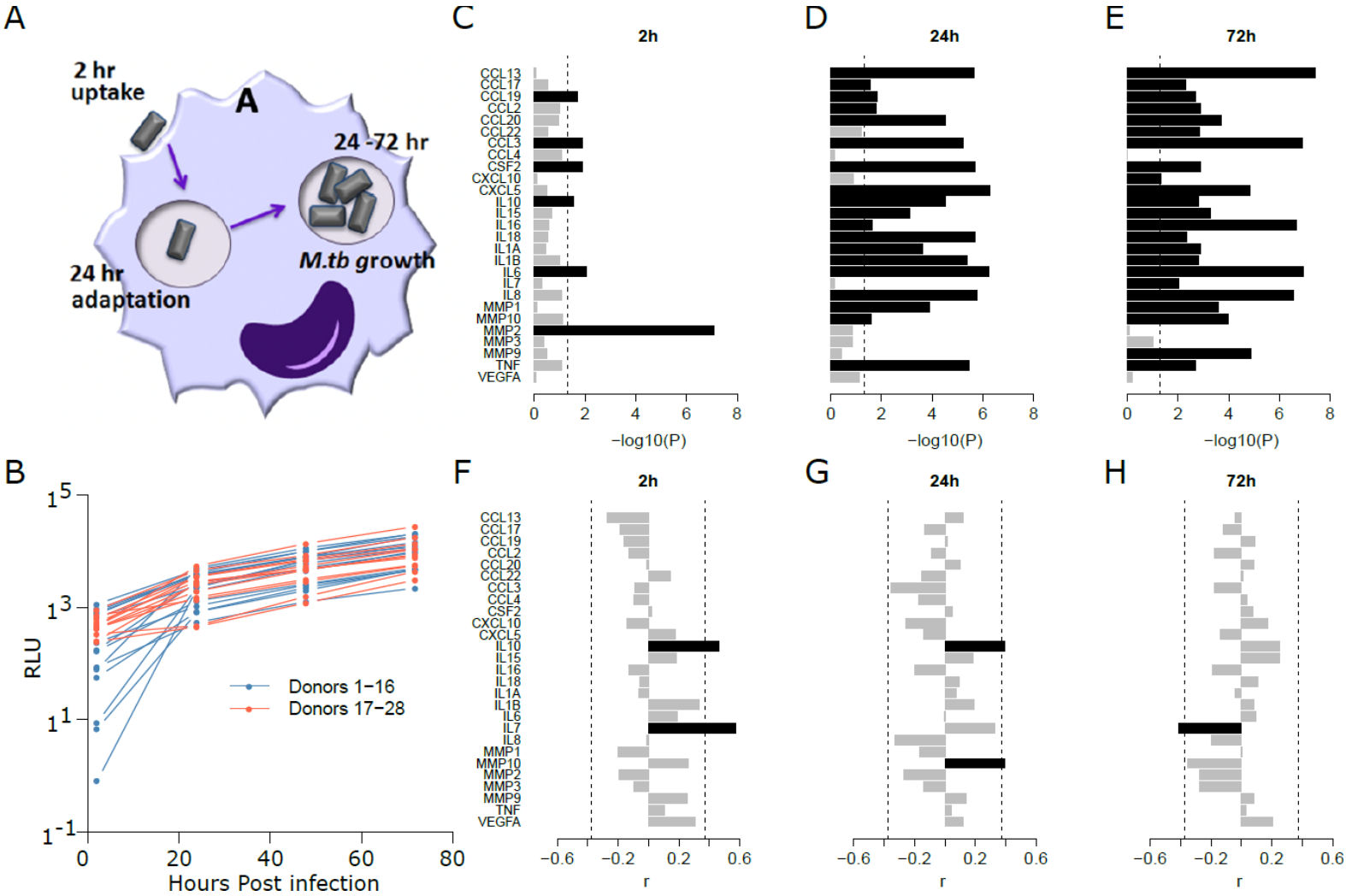

Figure 1. Panel A. **Schematic of *M.tb* cell adhesion and uptake, adaptation and growth in human alveolar macrophages (AMs)**. **Panel B**. Changes in normalized luminescence RLU values over the course of *M.tb* infection. The x-axis shows hours post infection, with RLUs representing mostly uptake and adaptation at 2h and 24h, and growth rates (72h/48h) (data in Supplemental Table 2; results shown here are with MOI 2:1). **Panels C, D,** and **E**. Differentially secreted proteins post infection at 2, 24, and 72h respectively (infected/controls at each time point). The bars represent adjusted p values (-log10), with significant proteins shown with black bars. **Panels F, G,** and **H**. Correlations (R^2) between protein levels and *M.tb* generation time (time for doubling during 48 to 72h period). Positive R^2 values indicate that increased levels correlate with increased generation times, and *vice versa.*

Figure supplement 1. The transcriptional response of 28 human AM cultures to *in vitro* incubation and to *M.tb* infection.

114 infection, in all AMs over 72h (**Supplementary File 2**). At 2h, 6 of the 27 proteins
115 (22.2%) are significantly differentially produced after *M.tb* infection (**Figure 1C**),
116 increasing to 23 proteins (85.2%) at 72h (**Figure 1E**), all with increased secretion in
117 infected cells. Differential secretion varies over time, with IL6 and MMP2 displaying
118 highest levels at 2h, and IL6, CCL13, and CCL3 at 72h. Pronounced *M.tb*-stimulated
119 secretion of MMP2 only at 2h (without stimulated mRNA expression; not shown)
120 suggests a mechanism of rapid release from the cell rather than *de novo* transcription.
121 Pro-inflammatory mediators including IL1β, TNF, and IL6 display significant differential
122 secretion at all-time points, indicating their contribution to a pro-inflammatory reaction
123 to infection.

124 We then tested whether protein levels secreted from infected cells correlate with *M.tb*
125 generation times (**Figure 1F-H; Supplementary File 3**), with Pearson correlation
126 reaching r=0.57 (IL7 at 2h). Three proteins are significant (FDR adj. p values <0.05):
127 IL7 (2h, 72h), IL10 (2h, 24h), and MMP10 (24h). High IL10 levels correlate with longer
128 generation times (slower growth) (r=0.46 and 0.49 at 2 and 24h, respectively),
129 whereas IL7 has a positive r value (0.57) at 2h and a negative one (-0.41) at 72h (but
130 is present at only low levels). A similar trend occurs with MMP10. Opposite effects at
131 different time points highlight the changing *M.tb*-AM interactions occurring over time.
132 These results indicate that protein expression profiles over the first 3 days of infection
133 influence *M.tb*-AM interaction dynamics.

134 **Transcriptomes of uninfected control and *M.tb*-infected human AMs reveal**
135 **differentially expressed gene profiles**

136 Transcript profiles were assessed for each AM sample at 2, 24, and 72h post infection,
137 using AmpliSeq(Papp et al., 2018). At each time point, 10,000-14,000 mRNAs were
138 detectable, and reads per million (RPM) from replicate assays were highly correlated
139 ($r^2 \geq 0.99$), enabling sensitive detection of differentially expressed (DE) genes. A
140 principal component analysis (PCA) of all datasets from control and infected AMs
141 reveals that 52% of the variance in gene expression between time points resulted from
142 exposure to *ex vivo* culture conditions alone, while *M.tb*-induced RNA expression
143 changes are smaller but increase over time (**Figure 1 - figure supplement 1**).
144 To identify significant DE genes (FDR adjusted $p \leq 0.05$) specific to infection, we
145 analyzed RNA expression by comparing uninfected control cells to infected cells at
146 each time point(Papp et al., 2018). This yielded 62 DE genes at 2h, 2,177 at 24h, and
147 3,662 at 72h post infection (**Figure 2A**; **Supplementary File 4)**. Thirty-six DE genes
148 significant at all-time points (**Figure 3**) include those encoding inflammatory cytokines
149 (IL1A, IL1B, TNF) and chemokine receptors (*e.g.*, CCR7) characteristic of a spectrum
150 representing “M1 type” cell states. Gene set enrichment analysis of 72h DE gene
151 profiles, using gene co-expression modules previously identified during macrophage
152 differentiation(Xue et al., 2014), shows significant enrichment of M1-like modules
153 (**Figure 2B**). An independent assignment of M1- and M2-associated genes(Orecchioni
154 et al., 2019) reveals high overlap of DE genes at each time point with either M1 or M2
155 genes (**Figure 2C-F**), accounting for 44.0% of M1 genes and 34.0% of M2 DE genes
156 at 72h. Cell type deconvolution with Quantiseq on the RNAseq profiles(Finotello et al.,
157 2019) supports a strong shift to M1 macrophages in infected samples, peaking at 24h,

158 whereas the M2 cell type predominates at 72h in control AMs (**Figure 4A,B**). While

159 significant correlations between M1/M2 profiles and *M.tb* uptake/growth dynamics are

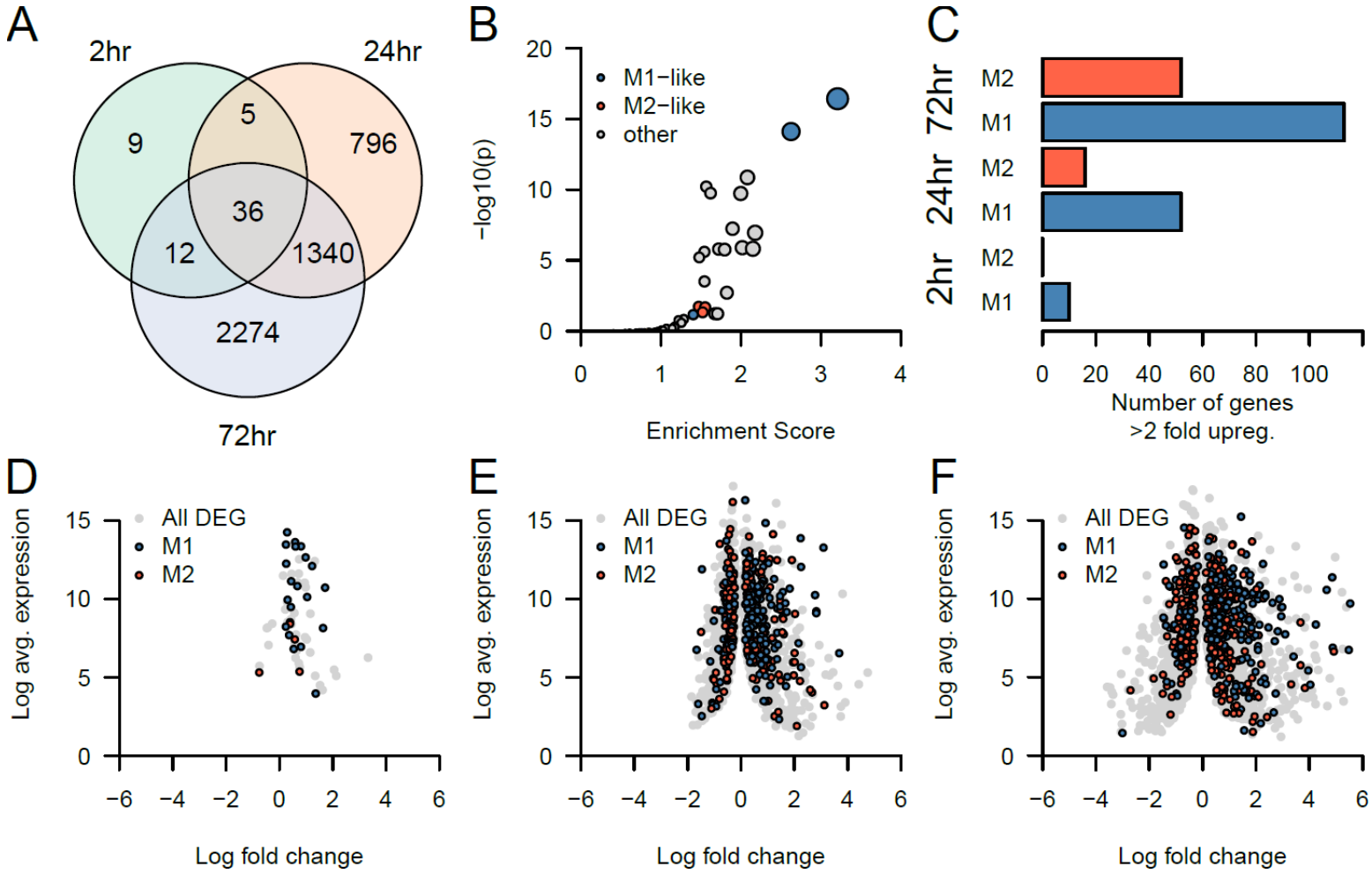

Figure 2. The transcriptional response of 28 human AMs to *M.tb* infection. **Panel A**. Venn diagram of differentially expressed (DE) genes between *M.tb*-treated and controls at three time points. Total number of genes with detectable expression (≥1RPM) was ~12,000. DE genes were detected with DESeq2 (adjusted p values <0.05): 62 at 2h, 2,177 at 24h, and 3,662 at 72h, with overlaps displayed in the Venn diagram. **Panel B.** Gene set enrichment analysis of DE genes from 72h using 48 gene expression modules previously determined as operational in macrophage differentiation. Modules annotated as 'M1-like' or 'M2-like' are shown in blue and red. **Panel C.** The number of DE genes with >2-fold upregulation defined as 'M1-like' or 'M2-like'. This uses an independent definition of M1-like and M2-like genes to (B). **Pane D-F:** Log_2 fold change and log_2 average expression for DE genes at 2h (D), 24h (E) and 72h (F). M1 and M2 genes are shown in blue and red respectively.

160

161 not detectable, individual donors vary significantly in the expression of several

162 characteristic M1 or M2 genes (**Figure 5**). As one example, STAT1 (a transcription

163 factor determining M1-like state) is one of the most differentially expressed genes

164 between infected and control macrophages at both 24h and 72h with an average of

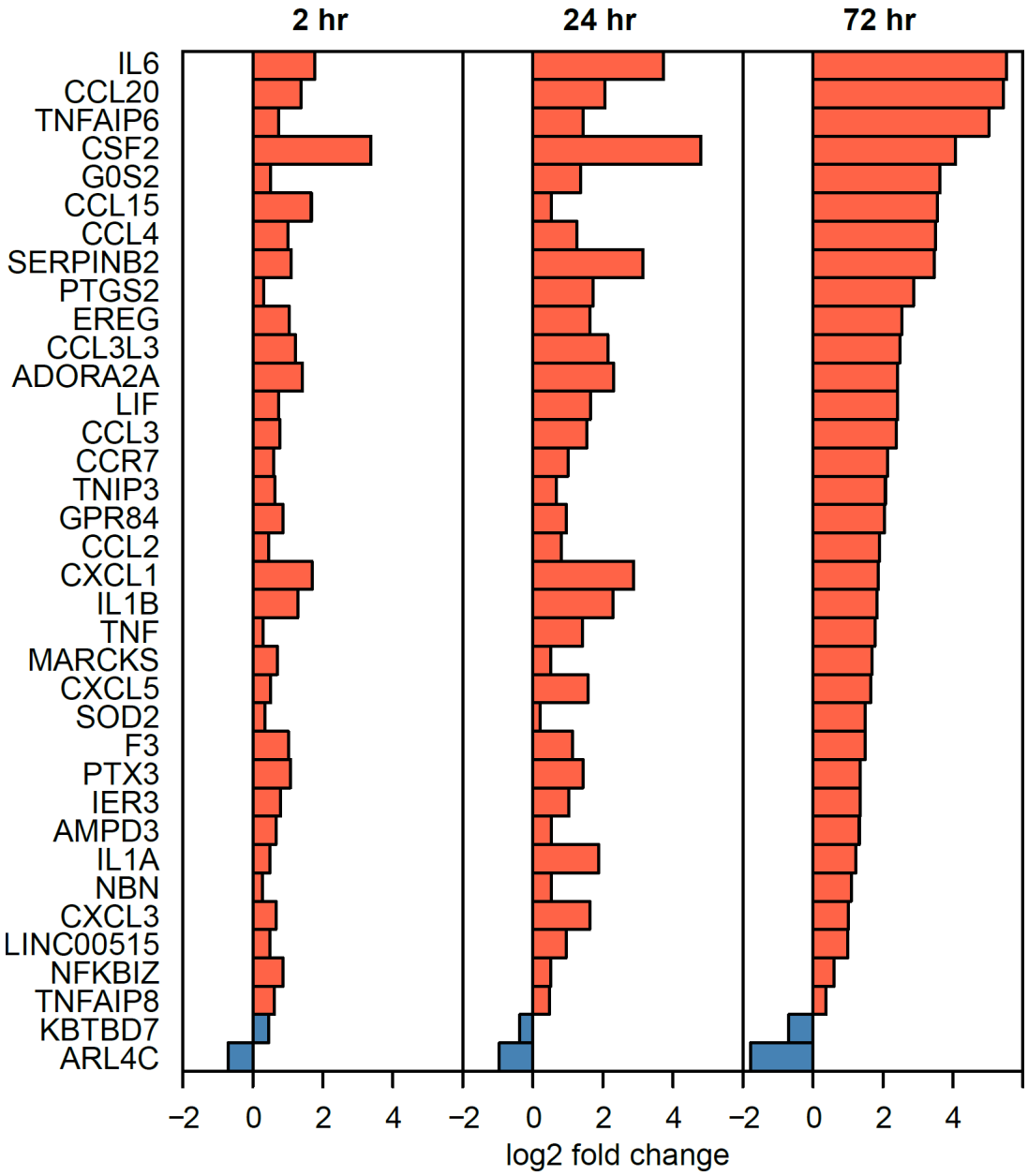

Figure 3. **The transcriptional response of 28 human AMs to *M.tb* infection.** Shown are the 36 significant DE genes common to all time points (see Figure 2A), and their $\log_2$ fold change.

165 >4-fold induction of gene expression over 72h, though induction varies between AM

166 donors from a 2-fold reduction to a 25-fold increase.

167

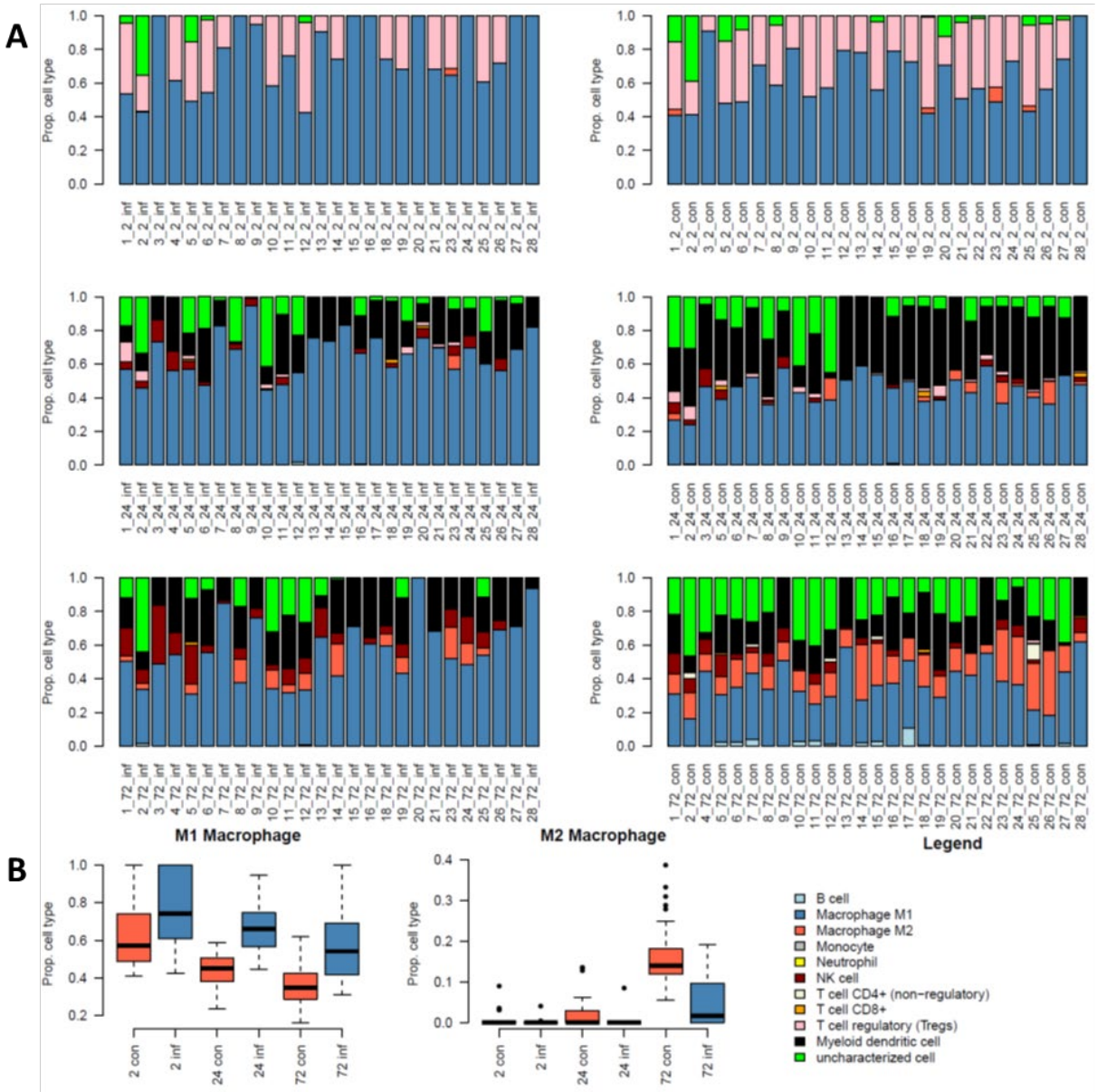

Figure 4. Cell type deconvolution with Quantiseq on RNAseq profiles at 2, 24 and 72h in infected and control cells. Panel A. Distribution of cell types visualized by the color code shown below. Note the preponderance of M1 type cells at 24h infected AMs, and of M2 type cells at 72h in controls. **Panel B.** Boxplots showing the proportion of M1 (left) and M2 (center) cells in infected and control cells at each time point, on the right is the legend for cell type proportions for the bar plots in (A).

168

169 **Differentially expressed genes (DE genes) displaying the most variable**

170 **expression among individual AMs (VE genes)**

171

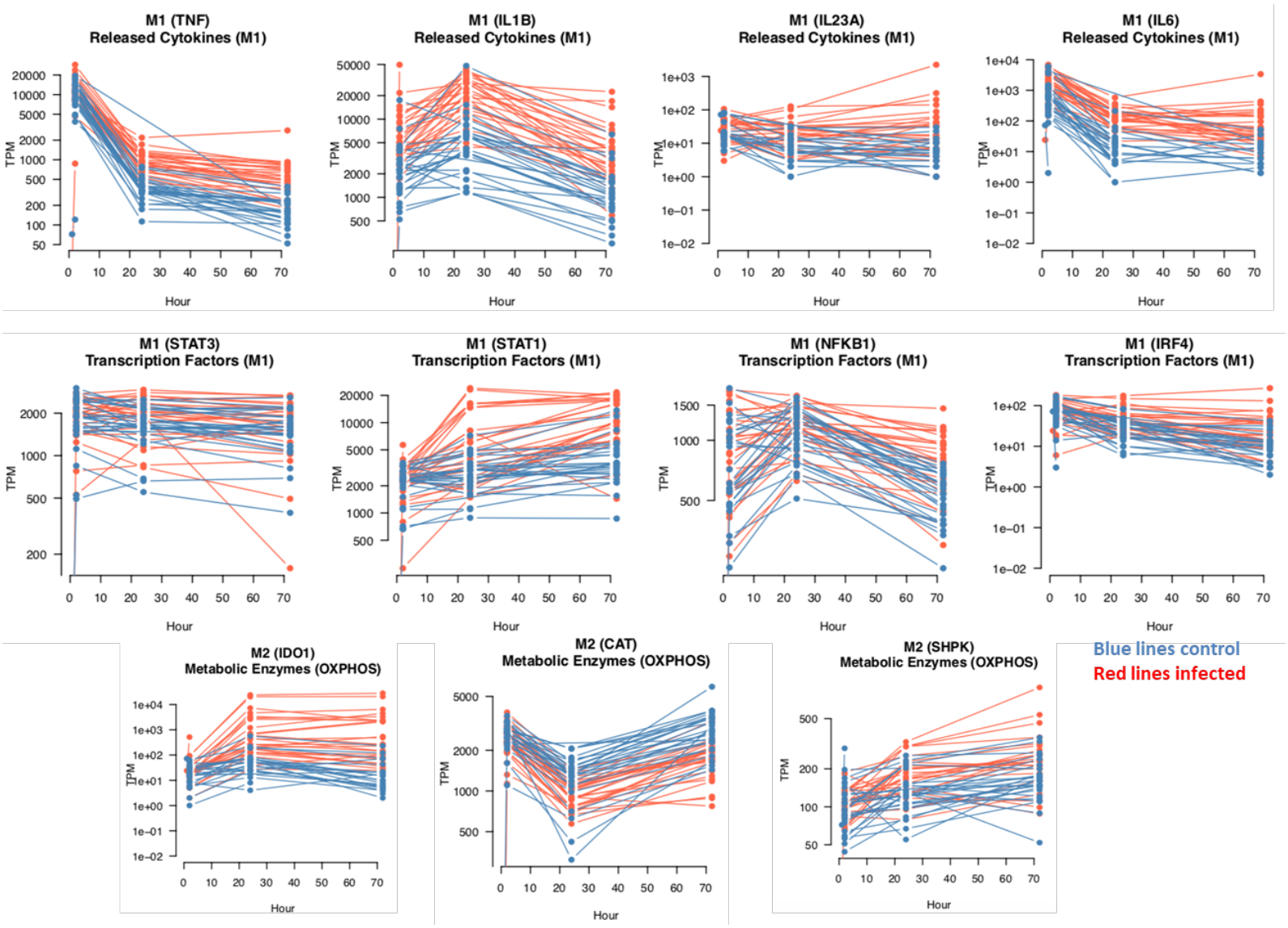

Figure 5. mRNA expression profiles over 72h in uninfected control and *M.tb*-infected AMs. The selected genes are marked as belonging to the M1 or M2 type macrophages, as annotated by other groups (Viola et al. 2019; Li et al. 2021), being involved in key metabolic differences between M1 and M2 types (categories: Transcription Factor, Surface Marker, Released Cytokine or Metabolic Enzyme, and sub categories such as M2A/M2B/M2C or OXPHOS/GLYCO.). https://www.ncbi.nlm.nih.gov/pmc/articles/PMC6618143/). See **Supplementary File 10.**

172

173 Genes with the most robust variable expression are of particular interest in
174 understanding inter-subject differences. We performed variance analysis of gene
175 expression in both control and infected AMs at all-time points, yielding a set of 324
176 genes with highly variable expression (VE genes; **Supplementary File 5A**). All 324 VE
177 genes are specific to the infected AMs, upregulated in infected cells, and also significant
178 DE genes (VE/DE genes). Examples include *IFI6, IL1B, CCL4, IDO1, GBP5, IRF1,*
179 *JAK3, UBD, CXCL,5, CCL20, VDR, CD80, IFI44L, NLRP3*, and *IL7R,* several of which
180 were previously implicated in TB pathogenesis. Correlations between expression of
181 these genes with *M.tb* generation times are listed in **Supplementary File 5A**. Several
182 genes (in RPMs) have strong correlations (r) with generation times, *e.g., MICAL2* (-0.69
183 at 24h), *RASSF2* (-0.73), *CD180* (-0.51), and *CNP* (0.49), the strongest correlations
184 associated with shortened generations times.

185 The extent of variable expression of the VE/DE genes is exemplified by the RNA
186 profiles across the 28 AMs (**Figure 6**). Among the VE/DE genes, expression of IDO1
187 mRNA is substantially stimulated by *M.tb* in only 10 of the 28 donor AMs (**Figure 6A**).
188 IL1B is more broadly expressed, but with high expression mostly coinciding with high
189 IDO1 expression (**Figure 6A**), similar to several other key genes (*e.g.*, IFNG, CXCL10,
190 UBD, IFI44L; **Figure 6B**). These most variably expressed VE/DE genes are likely
191 relevant to inter-individual variability following infection of AMs.

192 Reactome analysis yields several significant pathways, including Immunological
193 Diseases/Cellular Function and Maintenance/Inflammatory Response, and
194 Function/Immune Cell Trafficking (**Supplementary File 5B**). Ingenuity Pathway
195 Analysis (IPA) of the VE/DE genes yields the highest scoring hierarchical network with

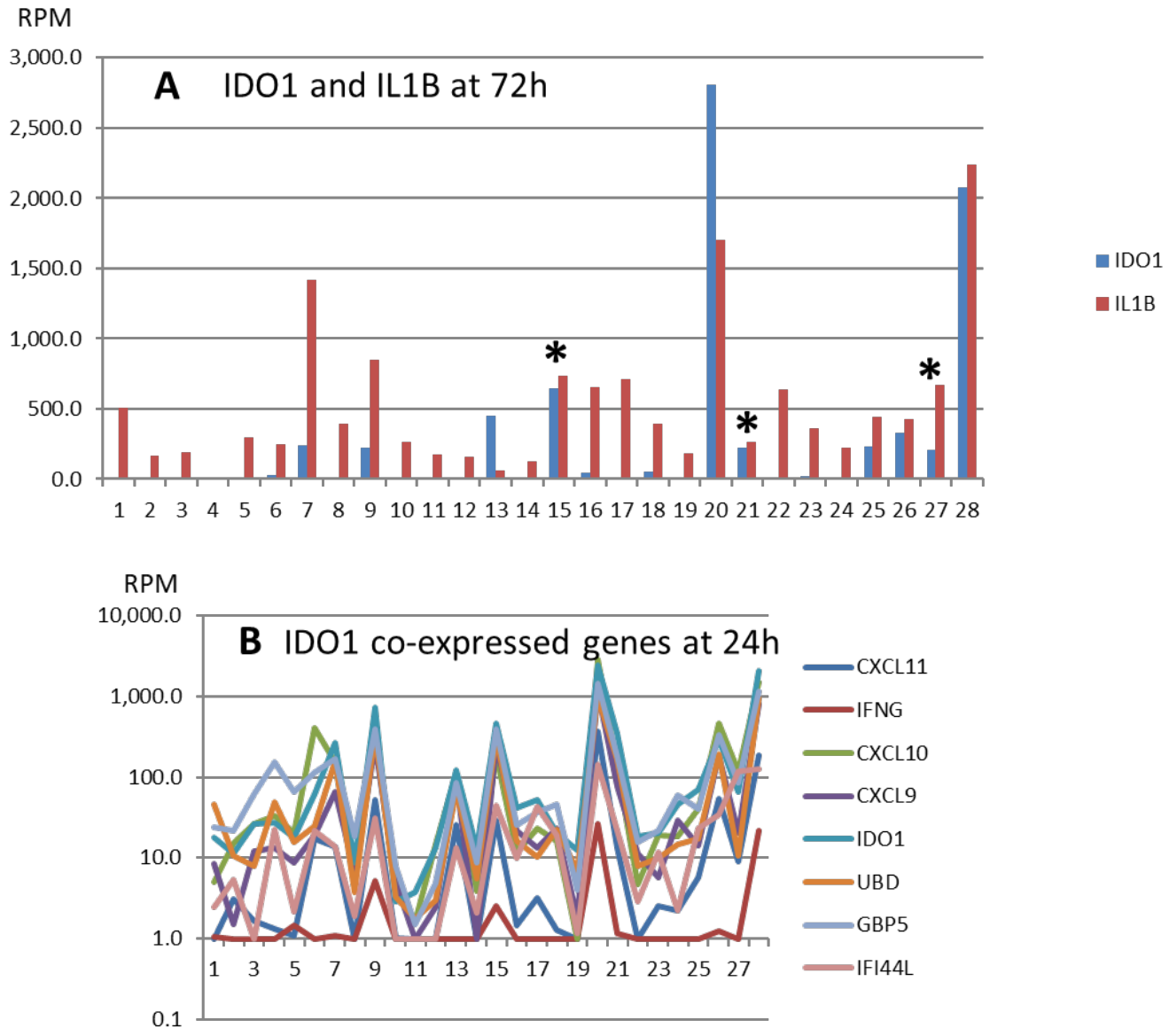

Figure 6. Expression of *IDO1*, *IL1B*, and co-expressed genes in AMs infected with *M.tb* over 72h. Panel A. Expression of *IDO1* and *IL1B*. Both are variably expressed with a different pattern across the 28 AMs. **Panel B**. Select mRNA transcripts with co-expression patterns similar to *IDO1*. *IDO1* is poorly expressed in 18 of 28 AMs (A), with tightly co-expressed genes representing the most variably expressed gene cluster (B).

197 IL1B at the top, and with STAT1, IRF1, and IDO1 as connected nodes (**Fig. 7,** full gene

198 annotation in **Figure 7 – figure supplement 1)**. Both *STAT1* and *IRF1* interact with the

199 *IDO1* promoter(Xue et al., 2012).

200

201

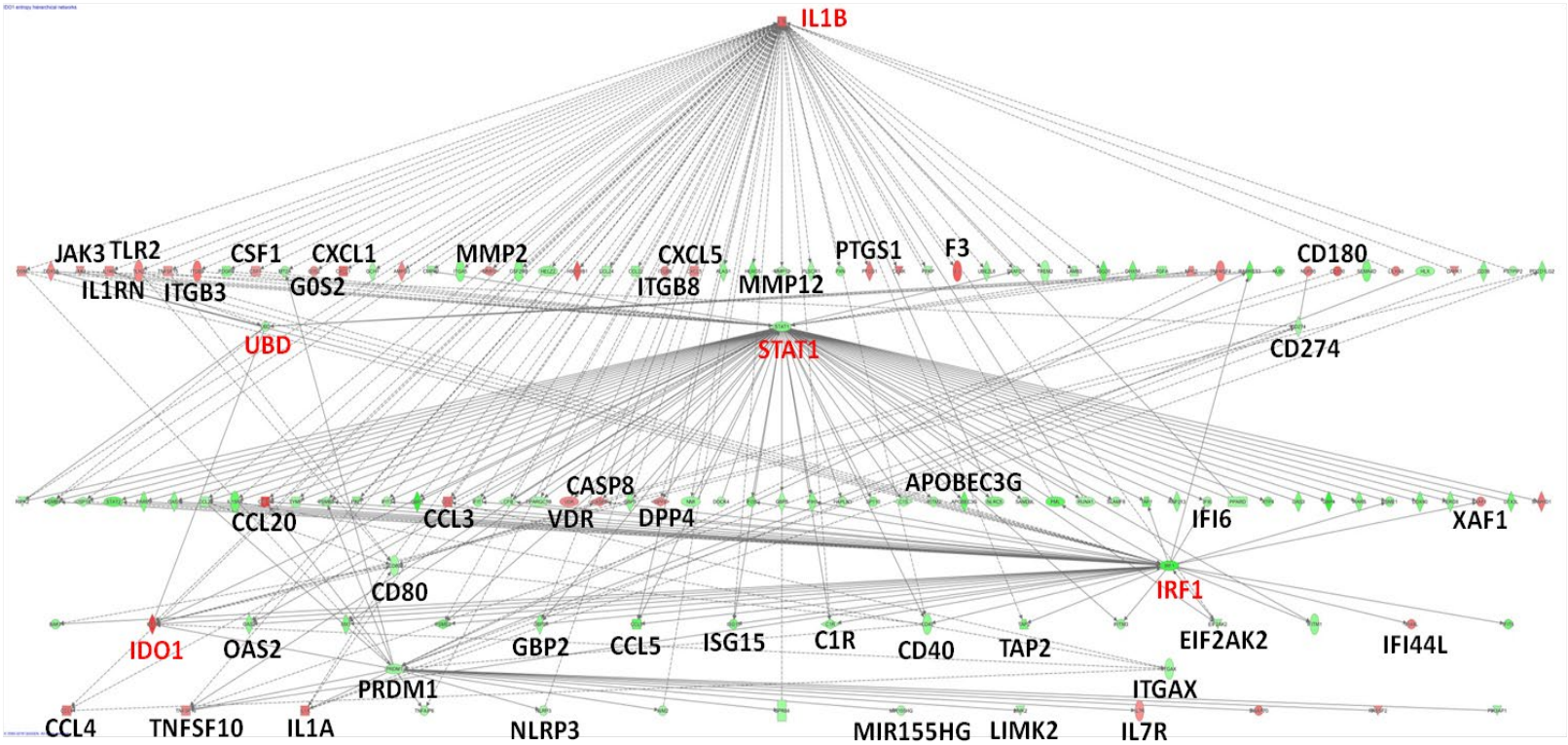

Figure 7. Network of DE genes with highly variable RNA expression (VE/DE genes). These VE/DE genes (n=324) were identified in the 28 AMs after *M.tb* infection across all time points. Standard pathway enrichment program, Ingenuity Pathway Analysis (IPA) (https://www.qiagenbioinformatics.com/products/ingenuity-pathway-analysis/), generates a top scoring gene network with *IL1B*, *UBD*, *STAT1*, and *IRF1* as key hub genes. *STAT1* and *IRF1* cooperatively bind to the promoter of *IDO1*, which is also highlighted (fully annotated network is depicted in Figure 7 – figure supplement 1). These key gene names are highlighted in red.

Figure supplement 1. Top scoring network of DE genes with highly variable expression (VE/DE genes).

202

203

204 **Identification of human AM genes associated with *M.tb* growth**

205 Single RNA profiles across the 28 donor AMs display high correlations with *M.tb*
206 growth dynamics but fail to yield significance upon FDR corrections. Several candidate
207 genes strongly correlate between RPMs at 24h and generation time, suggesting
208 biologically relevant relationships. To explore this further, we tested correlations
209 between *M.tb* generation times and gene expression modules, using WGCNA to build
210 three consensus networks using batch-corrected RNA profiles from infected and
211 control cells at 2, 24 and 72h, with RNAs having RPMs >35. This approach yielded
212 9,193, 9,098 and 9,115 genes, and identified 26, 27, and 37 modules for the 2, 24 and
213 72h time points, respectively (**Supplementary File 6A**). Correlation between network
214 eigengene modules for infected cells and *M.tb* generation times (during 48-72h) at 2,
215 24 and 72h identified four significant associations between bacterial growth rate and
216 eigengene modules, all in the 24h network (FDR-corrected p-value <0.05; blue r=-
217 0.52, yellow r=-0.61, red r=-0.55 and tan r=0.52; **Supplementary File 7,** columns D,E,
218 modules highlighted in red**).** Reactome pathway over-enrichment analysis
219 (**Supplementary File 8**) showed Processing and Metabolism of RNA, and DNA
220 Damage/Repair as significantly associated with these gene modules. Regulation of
221 genes involved in DNA repair and recombination had been linked to *M.tb* regrowth
222 from its non-replicating, persistent state(Du et al., 2016). This result supports a nexus
223 between gene networks and *M.tb* generation times.

224 To prioritize genes within significantly associated modules, we measured correlations
225 between generation time and gene expression for each gene within the four significant
226 modules (**Supplementary File 6B**, columns Q-V). We lowered the stringency of our

227 approach by performing multiple test correction based upon the module size, rather
228 than for all expressed genes. This approach yielded 143 significant genes, with 139
229 genes belonging to the yellow module in the 24h network (97.2%). The yellow module
230 genes have mostly negative correlations with generation times (117 of 139 genes,
231 84.2%); *i.e.,* elevated expression of these genes is associated with shorter generation
232 times (higher growth rates), perhaps signaling a key *M.tb*-induced AM response
233 favoring bacterial growth.

234 We performed hierarchical clustering of gene expression profiles and AM donors for
235 genes within the yellow module, limiting to genes where we find a significant correlation
236 between generation time and expression level (**Figure 8A**). This revealed four groups of
237 genes, two of which contain genes with a positive correlation to generation time
238 (clusters I and II), and two with a negative correlation to generation time (clusters III and
239 IV). Hierarchical clustering also identifies three groups of AM donors, groups 1 and 2
240 have significantly longer generation times compared to group 3 (**Figure 8B**)

241 Gene expression sub-groups display opposite profiles between groups 1 and 3, with
242 group 2 in between. We performed KEGG pathway enrichment of gene expression
243 clusters I and II (positively correlated with generation time) and clusters III and IV
244 (negatively correlated with generation time). This identified the TNF signaling pathway
245 as significantly enriched in negatively correlated genes (**Figure 8D**), and oxidative
246 phosphorylation and thermogenesis significantly enriched in positively correlated genes
247 **(Figure 8E)**. These results further support a biological relationship between gene
248 expression profiles and *M.tb* generation times.

249

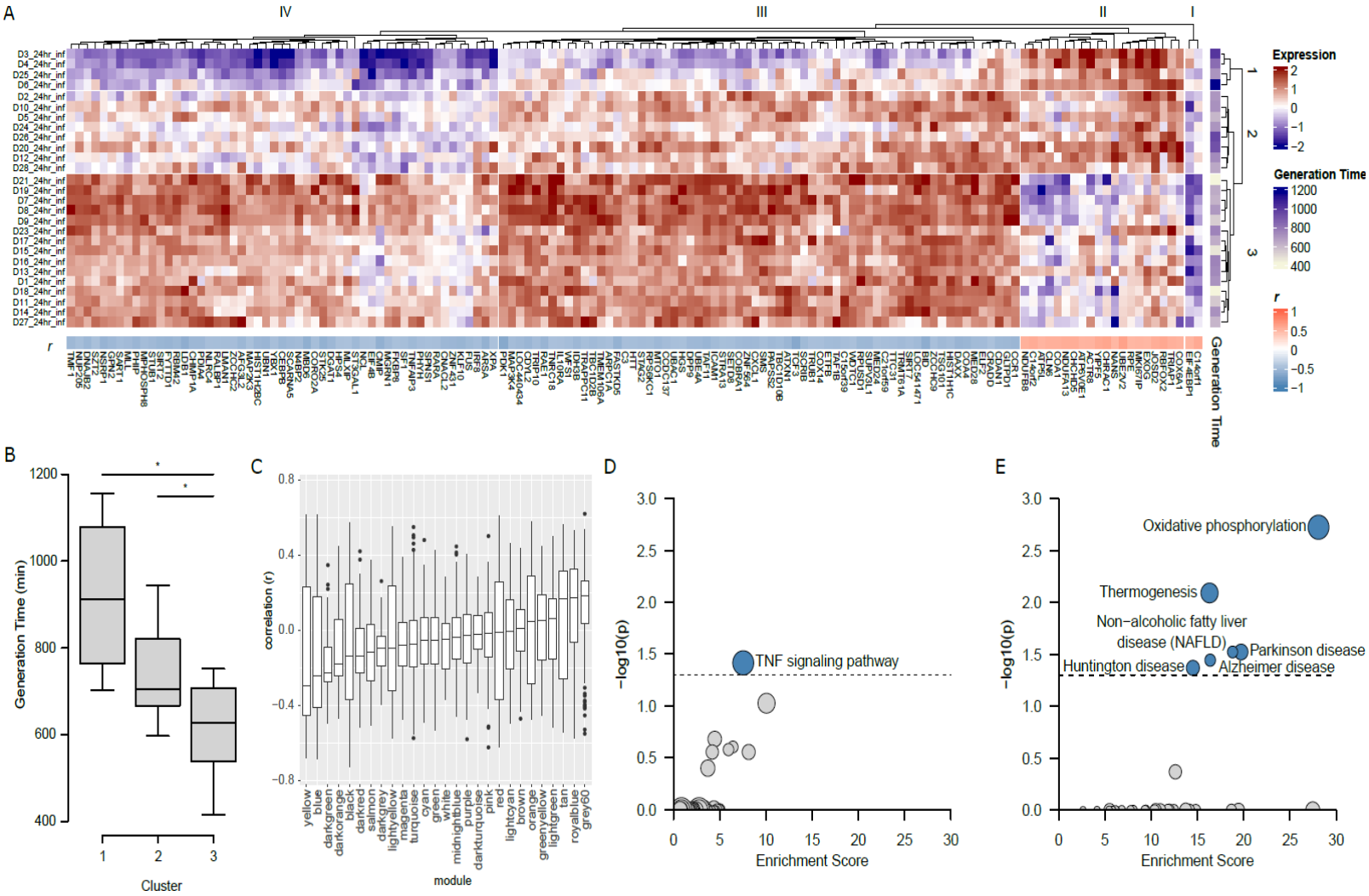

Figure 8. Association of the yellow gene module from 24h samples with generation time. (**A**) Gene expression profile of 139 genes from the yellow module which are correlated with generation time. Each gene is Z-normalized across all samples for ease of presentation (Expression). To the right of the heatmap is the generation time for each sample (Generation Time), and a dendrogram capturing the distance between samples. Below the heatmap are the r values for gene expression against generation time. Above the heatmap is a dendrogram capturing the distance between gene expression profiles. Three clusters of individuals were identified from the gene expression data (1-3). (**B**) The boxplot displays the generation time for individuals within each cluster; both cluster 1 and cluster 2 have significantly higher generation times than cluster 3. (**C**) The boxplot shows the distribution of r^2 values for all modules from 24h expression data. (**D**) KEGG pathway enrichment for negatively correlated genes (clusters III and IV). (**E**) KEGG pathway enrichment for positively correlated genes (clusters I and II).

Transcriptional modules coordinating the secreted protein response to *M.tb* infection in human AMs

252 Among the measured proteins implicated in TB pathogenesis, IL7, IL10 and MMP10
253 are significantly correlated with bacterial growth (Figure 1). In addition, the other
254 measured proteins have also been shown to impact disease progression through
255 interactions with the immune system not captured in our *in vitro* system. To identify the
256 transcriptional modules that may regulate or respond to these proteins, we assessed
257 correlations between eigengene modules and secreted protein levels (**Supplementary**
258 **File 9**), identifying 29 significant correlations after Bonferroni correction. Only 6/29
259 significant correlations are in non-infected control AMs, 3 of which are at the 2h time
260 point where there is little divergence in gene expression between control and infected
261 conditions. Of these, CCL3 expression is strongly correlated with the royal blue
262 module [**Supplementary Files 8** (column b) **and 9**], suggesting that the preexisting
263 expression profile in non-infected AMs may affect *M.tb* generation times.

264 In the 24h network, we find three modules with a significant link to both growth rate
265 and protein expression **(Supplementary Files 6B and 7)**. These are CCL3 (blue, red
266 and yellow modules) and IL10 (red module). Significant correlations between these
267 gene modules and individual proteins also suggest a causative relationship between
268 gene expression and *M.tb* growth.

269 At 72h, a single gene expression module (tan) correlates with the expression of
270 multiple proteins (IL15, IL18, IL1A and TNF). This module overlaps substantially with
271 our highest scoring network from IPA analysis of variably expressed VE/DE genes
272 (**Figure 7 – figure supplement 1**) with 47 of 184 module eigengenes (25.4%) falling
273 within this network, including *IDO1*, *IL1A* and *IL1B.*
274

275 **Discussion**

276 This study confirms large inter-individual variation in interactions between human AMs
277 and a single virulent strain of *M.tb* (Figures 1 and 2), and for the first time dissects
278 biological mechanisms underlying individual differences. Sousa et al.(Sousa et al.,
279 2020) had demonstrated that secretion of IL1B is a surrogate marker distinguishing
280 between TB cases with mild disease and severe TB, attributing differences in IL1B
281 induction to virulence of the strains tested, independent of the host. However, here we
282 show that a single virulent *M.tb* strain elicits substantial differences in IL1B expression
283 between individual AMs, highlighting host factors, with IL1B one possible predictive
284 marker of TB susceptibility.

285 The nexus between secreted TB candidate proteins and eigengene modules further
286 supports the finding that gene expression networks, both in uninfected and *M.tb*-
287 infected cells, affect early *M.tb*-AM interactions. While we have applied stringent FDR
288 adjustments to reveal significant correlations, strong candidate genes and networks
289 can serve to extract a deeper understanding of the various phases of *M.tb*-AM
290 interactions and their possible significance in the pathogenesis of TB.

291 We first measured 27 candidate proteins that are secreted by *M.tb*-infected AMs and
292 uninfected controls, finding robust stimulation by *M.tb* and inter-subject differences
293 (Figure 1 C-H). Importantly, three proteins (IL7, IL10, and MMP10) are significantly
294 correlated with bacterial growth over 48-72h (Supplementary File 3), supporting the
295 hypothesis that proteins relevant to TB pathogenesis affect early *M.tb*-AM interactions,
296 possibly presaging individual susceptibility to TB.

297 RNA expression profiles also appear to reflect or influence *M.tb*-AM interactions. The
298 precision of the AmpliSeq RNA assay, together with use of control AM expression at
299 each time point(Papp et al., 2018), enabled sensitive detection of numerous DE RNAs
300 across the 28 AMs (Figure 2; Supplementary File 4). DE genes significant at each time
301 point (Fig. 3) are consistent with previously reported results (*e.g.,* (Papp et al., 2018,
302 Zak et al., 2016, Moreira-Teixeira et al., 2020)), including inflammatory cytokines CSF2,
303 IL6, IL1B, and IFNG, but also anti-inflammatory factors such as CCL22. Gene Ontogeny
304 (GO) Pathway analysis reveals the expected prevalence for Innate Immune System,
305 Cytokine Signaling in Immune System, and more. The DE genes include both a
306 classically activated M1 type induced by inflammatory agents (*e.g.,* IFNG) and
307 alternatively activated M2 type induced by IL4 and IL13(Roy et al., 2018). While M1 and
308 M2 markers vary between individuals, the M1 type is strongly activated at 24h post
309 infection, while M2 markers increase at 72h, in particular in the uninfected cells (Figure
310 4). The balance of this mixed mode of activation may account in part for inter-subject
311 differences in *M.tb*-AM interactions, but no significant trends are observed. In previous
312 reports, *M.tb* ESAT-6-induced macrophage polarization to M1 phenotype occurred
313 early, then switching to M2 phenotype at a later stage of infection(Refai et al., 2018). In
314 our study, a substantial switch to the M2 phenotype at a later stage (72h) was observed
315 in uninfected control macrophages compared to infected AMs, which could be due to
316 increased expression of MMPs in control cultures. Upregulation of certain MMPs was
317 found to be associated with macrophage polarization to both M1 and M2 phenotypes in
318 *M.tb*-infected, cigarette smoke-exposed macrophages(Le et al., 2020).

319 Among the gene co-expression modules, one (yellow) significantly correlates with *M.tb*
320 generation times and, in addition, contains numerous individual genes that also
321 significantly correlate with *M.tb* growth (Supplementary File 6). As most correlations are
322 negative, these genes appear to favor *M.tb* growth. The module GO terms indicate
323 influence over translation processes, a potential mechanism by which *M.tb* usurps the
324 cellular machinery to its advantage.

325 Variably expressed (VE) genes can reveal markers of individual susceptibility or
326 resistance to disease phenotypes(Li et al., 2018), tested here for *M.tb* infection of AMs.
327 We find that all of the most robust VE genes also classify as DE genes, likely
328 contributing to the fate of *M.tb* in the cells. Prominent examples of VE/DE genes encode
329 IL1B and IDO1 (Supplementary File 5), suggesting that VE/DE genes are relevant to
330 infection and disease progression. IPA analysis of VE/DE genes yields Interferon
331 Signaling as the top pathway, and a network with IL1B, STAT1, and IRF1 as dominant
332 hubs including genes previously implicated in the cellular response to *M.tb* (e.g.,(Zak et
333 al., 2016, Moreira-Teixeira et al., 2020, Rothchild et al., 2019)) (Figure 7; Figure 7 –
334 figure supplement 1). This IL1B-dominated network connects IL1B, STAT1, and IRF1 to
335 IDO1, consistent with previous reports that the IRF1/STAT1 transcription complex binds
336 to the *IDO1* promoter(Xue et al., 2012, Du et al., 2000). IDO1 has been proposed
337 recently as a sensitive and selective biomarker for active TB(Adu-Gyamfi et al., 2017).
338 Its metabolic products, immunosuppressive kynurenins, act by preventing access of
339 cytotoxic T cells to infected macrophages in TB lung granulomas(Gautam et al., 2018).
340 IDO1 is robustly expressed in only 10 of 28 AMs after *M.tb* stimulation, with a similar
341 expression profile for IL1B, CXCL9-11, IFNG, UBD, IFI44L, and GBP5 (an IFN/IL1B

342 activated GTPase mediating antibacterial defense) (Figure 6). We propose that
343 expression of both IL1B and IDO1 could be early predictive biomarkers of susceptibility
344 to *M.tb* for a given individual.

345 The nexus we observe between secreted proteins reported relevant to TB and gene
346 expression modules, with overlap to variably expressed VE/DE genes and, on the other
347 hand, to *M.tb* generation times, strengthens our hypothesis that early *M.tb*-AM
348 interactions could signal an individual's susceptibility to infection and potentially risk of
349 overt TB.

350 In summary, our results identify known and novel key genes and their encoded
351 transcripts and proteins in the early phase of *M.tb* infection of freshly isolated human
352 AMs. Previous work shows that infection of macrophages with *M.tb* stimulates multiple
353 pathways, including both interferon type 1 and 2 pathways – thought to exert opposing
354 effects on infections(Roy et al., 2018, Rothchild et al., 2019). We show here that
355 variably and differentially expressed genes and their networks affecting *M.tb*-AM
356 interactions can account for inter-individual variability during the early phase of infection.
357 Results of this study provide a foundation for identifying predictive biomarkers of an
358 individual's susceptibility or resistance to *M.tb* infection, and response to vaccines and
359 therapeutics(Tameris et al., 2013).

360 *Limitations.* While the study group of 28 healthy AM donors was sufficient to reveal
361 significant genes associated with *M.tb*-AM interactions, our results require replication.
362 Larger cohorts will be needed to address contributions of single genes and networks to
363 uptake, adaptation, and growth, reveal genetic factors, and assess ethnicity, sex and
364 age, and environmental factors. Nevertheless, the study approach provides rich

365 datasets suitable to accelerating the development of predictive biomarker panels of an
366 individual's risk for TB. The design of our study precluded repeat measures from each
367 donor. However, our longstanding studies with healthy donor human monocyte-derived
368 macrophages has demonstrated that individual donors provide consistent results for
369 comparable measurements over time.
370

371 **Materials and Methods**

372 **Measurements of uptake, adaptation, and growth rate of *M.tb* in infected AMs**

373 Fresh AMs were obtained within 6h from 28 tuberculin skin test (TST)-negative
374 healthy donors from Caucasians, Asians, Africans, according to the demographics of
375 the Columbus, Ohio area (**Table 1**), under an approved IRB protocol at the Ohio State
376 University Wexner Medical Center. Isolation and culture of human AMs from
377 bronchoalveolar lavage (BAL) was done as described(Gaynor et al., 1995, Nguyen et
378 al., 2012). Briefly, BAL fluid was centrifuged and washed once in cold RPMI at 4^0C,
379 and the cell pellet was re-suspended in RPMI medium. A portion of the cell
380 suspension was subjected to cytospin followed by staining and microscopy to
381 determine macrophage content (94 ± 5%; mean ± SD, N=10). AMs were adhered in
382 either a 24-well plate ($1.5x10^5$ cells/well) or 96-well plate ($5x10^4$ cells/well) in RPMI
383 containing 10% human AB serum and Penicillin G (10,000 U/ml) for 2h (99% pure)
384 before collecting the supernatants and washing/lysing the adhered cell monolayer, in
385 part used for protein and RNA analysis, respectively. Then, medium was replaced
386 and incubations continued until 24 and 72h to repeat protein and RNA analysis.
387

388

Table 1. Donor demographics of AM samples used in this study (n=28)

Donor	Sex	Age (Years)	Race	Donor	Sex	Age (Years)	Race
D1	Female	24	Asian (Chinese)	**D15**	Male	18	Hispanic
D2	Male	24	African-American	**D16**	Female	25	Caucasian
D3	Male	27	Caucasian	**D17**	Female	20	Caucasian
D4	Female	26	Caucasian	**D18**	Female	26	Caucasian
D5	Female	26	Caucasian	**D19**	Male	19	African-American
D6	Male	21	Caucasian	**D20**	Female	22	Hispanic
D7	Male	24	Caucasian	**D21**	Male	20	Asian (Chinese)
D8	Female	22	Caucasian	**D22**	Female	19	Not stated
D9	Male	23	Caucasian	**D23**	Female	19	Caucasian
D10	Male	21	Caucasian	**D24**	Male	23	Caucasian
D11	Female	46	Caucasian	**D25**	Male	24	Hispanic
D12	Female	22	African-American	**D26**	Male	23	Caucasian
D13	Male	27	Asian (Indian)	**D27**	Female	20	Caucasian
D14	Male	33	Asian (Chinese)	**D28**	Female	19	Caucasian

Male/Female = 14/14; Caucasian = 60% (17/28), Asian = 14% (4/28), African-American = 11% (3/28), Hispanic = 11% (3/28)

389

390 Virulent *M.tb* $H_{37}R_v$ single cell suspensions were prepared(Schlesinger et al., 1990).

391 The virulent *M.tb* strain used contains the entire bacterial Lux operon cloned in a

392 mycobacterial integrative expression vector (*M.tb* $H_{37}R_v$-Lux) as described(Salunke et

393 al., 2015). *M.tb* cellular uptake, adaptation, and intracellular growth were assessed as

394 relative luminescence units (RLUs) at 2, 24, 48, and 72h in 3-5 wells for each

395 condition (mean values of 3-5 technical replicates are provided for each donor) using
396 a multiwell plate reader Glomax (Promega). Each 2h incubation was performed at a
397 multiplicity of infection (MOI) of both 2:1 and 10:1 (*M.tb/*AM cells for RLU assays);
398 RNA and protein was measured only with MOI of 2:1.

399 For technical reasons, AM uptake and growth assays from donors 1-16 were
400 incubated in 24 well plates, while AMs from donors 17-28 were incubated in 96 well
401 plates. Use of the different plates resulted in ~3-fold difference in mean RLUs
402 between the two sets of donor groups (directly related to a different number of
403 AMs/well). For all analysis we performed batch correction of protein, transcript and
404 growth rate measures using ComBAT(Johnson et al., 2007) to remove the impact of
405 different plates used during culture as such we specified the batches as individuals 1-
406 16 and 17-28.

407 **Measurement of secreted proteins in control and *M.tb*-infected AMs**

408 Supernatants from culture wells of uninfected and infected AMs from 28 donors at 2,
409 24, and 72h were analyzed for secreted proteins relevant to *M.tb*-macrophage
410 interactions using multiplex kits from Meso Scale Discovery (MSD) (Rockville, MD).
411 The supernatants were collected at 2h and replaced with fresh medium, followed by
412 continuing incubation until 24 or 72h. Twenty-seven secreted proteins were
413 measured: 4 inflammatory mediators (TNF-α, IL-6, IL-1β, IL-10; V-PLEX kit), 6
414 cytokines [CSF2 (GM-CSF), IL-15, IL-16, IL-1α, IL-7, VEGFA] and 12 chemokines [IP-
415 10 (CXCL10), MCP-1 (CCL2), MCP-4 (CCL13), MDC (CCL22), IL-8, TARC (CCL17),
416 MIP-1α (CCL3; U-PLEX (customized multiplexing), MIP-1β (CCL4), ENA-78 (CXCL5),

417 IL-18, MIP-3α (CCL20), MIP-3β (CCL19)], and 5 matrix metallo-proteinases (MMP-1,
418 MMP-2, MMP-3, MMP-9, MMP-10; MMP 3-PLEX and MMP 2-PLEX).

419 **Measurement of RNA expression from uninfected and *M.tb*-infected human AMs**

420 Expression of 20,804 RNAs, including 2,228 non-coding RNAs (ncRNAs), was
421 measured with AmpliSeqTM (Whole transcriptome Human Gene Expression Kit, Life
422 Technologies) for 28 donor AMs at 2, 24, and 72h after infection, for both uninfected
423 controls and infected AMs at each time point (MOI 2:1). AmpliSeq transcriptome
424 analysis incorporates a targeted, amplicon-based (~110 bps, spanning exons)
425 workflow, and is quantitative over orders of magnitude. The precision of AmpliSeq
426 analysis detects *M.tb*-induced expression changes with high sensitivity in human
427 MDMs and AMs infected with *M.tb*(Papp et al., 2018). Genomic DNA and total RNA
428 (TRIzol® Reagent (Ambion™, Austin, TX)) were prepared from AMs using published
429 procedures(Azad et al., 2013). RNA was purified, DNase-treated, RNA concentration
430 measured, and RNA integrity assessed as described(Papp et al., 2018). After reverse
431 transcription of 10 ng total RNA, using the AmpliSeq primers with the SuperScript®
432 VILO™ cDNA Synthesis kit. the cDNAs were amplified for 12 cycles with Ion
433 AmpliSeq™ primers and barcoded adapters, resulting libraries purified and pooled in
434 equal amounts for emulsion PCR on an Ion OneTouch™ 2 instrument, followed by
435 sequencing with the Ion Proton™ sequencer(Papp et al., 2018). Reads were aligned
436 to BED (Browser Extensible Data) file specific for AmpliSeq amplicons. Typically, we
437 obtain 5-9 million mappable reads per sample, with ~50-60% of RNA targets
438 detected(Papp et al., 2018). Repeat experiments in the same sample yield correlation
439 values of r^2>0.99 (for both independent replicates and sequencing chip replicates).

440 The AM sample from D17 at 2h and 72h yielded <1 million reads and were excluded
441 from the analyses. The AmpliSeq reads were normalized to mapped fragments per
442 million reads for quantifying transcript expression levels(Mortazavi et al., 2008),
443 yielding relative abundance for predicted transcripts in each AM.

444 **Differentially-expressed (DE) genes between control and *M.tb*-infected human**
445 **AMs**

446 To identify DE genes, we employed DESeq2(Love et al., 2014). FDR adjusted p
447 values of 0.05 were used as cutoff for identifying DE genes at each time point. We
448 estimated size factors using the "poscount" approach to correct for different
449 sequencing depth and performed independent analysis at each time point, specifying
450 the individual/donor and condition (infected or control) in the model.

451 **Weighted gene co-expression network analysis) (WGCNA)**

452 We derived three gene co-expression works using WGCNA(Langfelder and Horvath,
453 2008) with the following parameters; power=8, TOMtype=signed, minModuleSize=30,
454 mergeCutHeight=0.25, minKMEtoStay=0. These were blockwise consensus modules
455 with the gene expression data from the control and infected cells grouped
456 independently. We correlated the module eigengenes to either bacterial growth rate, or
457 to proteins expressed/secreted from the same time point and performed FDR correction
458 on p values.

459 **Detection of genes with variable expression in control and *M.tb*-infected AMs,**
460 **characterized by variance measures**

461 To identify the most variably expressed RNAs in control AMs and in those separately
462 after *M.tb* infection, all AM transcriptome data at each time were subjected to Levene's

463 test(Levene, 1960), with ratios of variances as test statistics, reported adjusted p-value
464 (FDR) for selected RNAs. A second variability test assesses whether the entropy of a
465 given RNA's expression is higher than expected given the total entropy in the *M.tb*-
466 treated AMs(Handelman et al., 2015). A permutation test yields p-values for significance
467 of the entropy computations.

468 **Gene pathway and ontogeny analysis.** We performed over representation analysis of
469 gene ontology (GO) terms and reactome pathways using WebGestalt(Liao et al., 2019)
470 taking the relevant gene lists for each comparison as an input and using default
471 parameters. We retained GO terms or pathways which reached an FDR corrected p
472 value of 0.05. Comparison to genes associated with M1 and M2 states was performed
473 using a curated list of genes from Viola et al.(Viola et al., 2019) and Li et al.(Li et al.,
474 2021).

475

476 **Acknowledgements**

477 This study was supported in part by a grant from the Bill & Melinda Gates Foundation,
478 and a grant from the National Institutes of Health (NIH) General Medical Sciences U01
479 GM092655.

480

481 **Competing Interests**

482 The authors declare no competing interests.

483

484 **Supplementary Files:**

485 **Supplementary File 1. Relative *M.tb* Luminescence Units (RLUs) and RLU ratios**
486 **between time points.** All 28 AMs were incubated for 2h with *M.tb* at MOI 2:1 and 10:1,
487 and luminescence was measured at 2, 24, 48, and 72h (n=3 per sample and time

488 point). The RLU profiles were similar between MOI 2:1 and 10:1; therefore, only MOI
489 2:1 values are shown. To estimate *M.tb* generation times (equivalent to growth rates)
490 between 24, 48, and 72h, RLU ratios between time points were calculated with
491 unadjusted RLUs, yielding similar results with MOI 2:1 and 10:1, indicating the ratios are
492 robust and reproducible.

493 **Supplementary File 2. Protein (n=27) levels secreted into the culture medium**
494 **during 2, 24, and 72h incubation of uninfected AMs (Con) and after infection with**
495 ***M.tb* (Mtb) from 0-2h incubation.** The incubation medium was changed once at 2h.
496 Results are in picogram/ml, secreted into the medium by AMs over the incubation
497 periods 0-2h, 2-24h, and 2-72h. Each value is the mean of results from duplicates of
498 each of 2 independent samples per AM.

499 **Supplementary File 3. Correlations between secreted proteins and *M.tb***
500 **generation time during the 48 to 72h incubation period.** All values are r correlations,
501 with + or – indicating whether the correlation is positive (longer generation time) or
502 negative (shorter generation time).

503 **Supplementary File 4. Differential expression of RNAs control *versus M.tb***
504 **infected AMs in all 28 donor AMs at 2h, 24h and 72h (Suppl. Files 4A, B, and C),**
505 **using separate non-infected control AMs for each time point.** baseMean: log2
506 RPMs in control cells at each time point; log2FoldChange: RPM ratios of
507 infected/control. lfcSE: log fold-change standard error, stat: test statistic from DESeq2;
508 pvalue: unadjusted p values. padj: FDR-adjusted p value.

509

510 **Supplementary File 5: A. Variably expressed genes (VE genes).** RNAs displaying
511 the most variable expression between AMs based on variance and entropy in AM
512 controls and *M.tb*-treated cells. All of the most variably expressed genes (VE Genes)
513 were also significant DE genes (VE/DE genes), hence ordered in decreasing DE Expr
514 Log2 Ratios (column C). All samples at all-time points were subjected to Levene's test
515 (using ratios of variances as a test statistic) (Levene, 1960) to find RNAs that are
516 differentially variable between control samples and *M.tb* stimulated AMs, yielding RNAs
517 with highest variance in cases that are induced (or inhibited) by *M.tb* stimulation only in
518 a subset of individuals (encoded by VE genes). A second analysis asked whether the
519 entropy of RNA expression in the *M.tb*-treated group is higher than expected given the
520 total entropy over all AM samples (Handelman et al. 2015), using a permutation test to
521 yield p-values for significance of the entropy computations. tau ratios are ratios of
522 standard deviations (non-treated/treated). FDR Levene and FDR entropy are the
523 respective adjusted p values. Columns I, J, and K present correlation values (r, red
524 positive, blue negative) for each VE/DE gene with generation time over 48-72h (as in
525 Suppl. File 3), using RPM expression values for each gene at 2, 24, and 72h in infected
526 AMs. **B. Reactome Pathways significantly overrepresented among VE genes.**
527 Results are from reactome.org/PathwayBrowser using 324 VE/DE genes.
528 **Supplementary File 6: A. Network module gene membership and correlations**
529 **between RNA expression (log2 RPMs) at 2, 24 and 72h in infected cells, and *M.tb***
530 **generation times** (*aka* RLU ratios, growth rates, 48-72h) in *M.tb* infected and control
531 AMs. **B. Genes with a significant association between growth rate and expression**
532 **after FDR correction within modules.** Correlations are as indicated in Supplementary

533 Files 3 and 5. The yellow module itself (24h RPMs) is also significantly correlated with
534 generation time.

535 **Supplementary File 7. Summary of significant correlations between protein levels**
536 **and gene modules in control and infected AMs at 2, 24 and 72 h.** Significant module
537 correlations with generation time are also indicated (blue, red, tan, yellow; 'yes'; column
538 D). CCL3 is present in multiple modules. Negative correlations are highlighted in red**.**
539 Adjusted p values reflect the number of proteins (n=27) and number of modules.

540 **Supplementary File 8. GO term enrichment for 72hr gene modules.** These four
541 modules (blue, yellow, tan red) are significantly correlated with *M.tb* generation times
542 (see Suppl. File 6). Results are from http://www.webgestalt.org/.

543 **Supplementary File 9: A-F. Correlations between protein levels and gene**
544 **modules in control and infected AMs at 2, 24 and 72 h.** Shown are correlations (r,
545 upper panels) and Adjusted p values (lower panels). Significant correlations are
546 highlighted. A few strong correlations occur in the uninfected cells (for example at 2h:
547 CCL3 with the Royalblue module (r=0.80, p=7.9e-7), CXCL5 with the Purple module
548 (r=0.72, p=3.7e-5), and IL6 with the Royalblue module (r=0.70, p=6.6e-6). Positive
549 correlations are highlighted in red, negative in blue (most in the infected AM
550 correlations)**.** Adjusted p values reflect the number of proteins (n=27).

551 **Supplementary File 10. Differentially expressed genes selected from a curated**
552 **M1/M2 macrophage gene list** (Table 1
553 in https://www.ncbi.nlm.nih.gov/pmc/articles/PMC6618143/). Listed are DE in our
554 dataset at any single time point. The genes are labelled as relevant to M1 or M2 state,
555 the gene name, and the broad category (Transcription Factor, Surface Marker,

556 Released Cytokine or Metabolic Enzyme) and sub categories such as M2A/M2B/M2C
557 or OXPHOS/GLYCO. Fold change pval and Fold change data are from Supplementary
558 Files 4A-C.
559
560
561 **References**

562 ADU-GYAMFI, C. G., SNYMAN, T., HOFFMANN, C. J., MARTINSON, N. A., CHAISSON, R. E.,
563 GEORGE, J. A. & SUCHARD, M. S. 2017. Plasma Indoleamine 2, 3-Dioxygenase, a
564 Biomarker for Tuberculosis in Human Immunodeficiency Virus-Infected Patients. *Clin*
565 *Infect Dis,* 65**,** 1356-1358.
566 AZAD, A. K., CURTIS, A., PAPP, A., WEBB, A., KNOELL, D., SADEE, W. & SCHLESINGER, L.
567 S. 2013. Allelic mRNA expression imbalance in C-type lectins reveals a frequent
568 regulatory SNP in the human surfactant protein A (SP-A) gene. *Genes Immun,* 14**,** 99-
569 106.
570 AZAD, A. K., LLOYD, C., SADEE, W. & SCHLESINGER, L. S. 2020. Challenges of Immune
571 Response Diversity in the Human Population Concerning New Tuberculosis Diagnostics,
572 Therapies, and Vaccines. *Front Cell Infect Microbiol,* 10**,** 139.
573 AZAD, A. K., SADEE, W. & SCHLESINGER, L. S. 2012. Innate immune gene polymorphisms in
574 tuberculosis. *Infect. Immun,* 80**,** 3343-3359.
575 BARREIRO, L. B., TAILLEUX, L., PAI, A. A., GICQUEL, B., MARIONI, J. C. & GILAD, Y. 2012.
576 Deciphering the genetic architecture of variation in the immune response to
577 Mycobacterium tuberculosis infection. *Proc Natl Acad Sci U S A,* 109**,** 1204-9.
578 BLISCHAK, J. D., TAILLEUX, L., MITRANO, A., BARREIRO, L. B. & GILAD, Y. 2015.
579 Mycobacterial infection induces a specific human innate immune response. *Sci Rep,* 5**,**
580 16882.

581 BRAGINA, E. Y., TIYS, E. S., RUDKO, A. A., IVANISENKO, V. A. & FREIDIN, M. B. 2016.
582 Novel tuberculosis susceptibility candidate genes revealed by the reconstruction and
583 analysis of associative networks. *Infect Genet Evol,* 46**,** 118-123.
584 COLDITZ, G. A., BREWER, T. F., BERKEY, C. S., WILSON, M. E., BURDICK, E., FINEBERG,
585 H. V. & MOSTELLER, F. 1994. Efficacy of BCG vaccine in the prevention of
586 tuberculosis: Meta-analysis of the published literature. *JAMA,* 271**,** 698-702.
587 DU, M. X., SOTERO-ESTEVA, W. D. & TAYLOR, M. W. 2000. Analysis of transcription factors
588 regulating induction of indoleamine 2,3-dioxygenase by IFN-gamma. *J Interferon*
589 *Cytokine Res,* 20**,** 133-42.
590 DU, P., SOHASKEY, C. D. & SHI, L. 2016. Transcriptional and Physiological Changes during
591 Mycobacterium tuberculosis Reactivation from Non-replicating Persistence. *Front*
592 *Microbiol,* 7**,** 1346.
593 FINAN, C., OTA, M. O., MARCHANT, A. & NEWPORT, M. J. 2008. Natural variation in immune
594 responses to neonatal Mycobacterium bovis Bacillus Calmette-Guerin (BCG)
595 Vaccination in a Cohort of Gambian infants. *PLoS One,* 3**,** e3485.
596 FINOTELLO, F., MAYER, C., PLATTNER, C., LASCHOBER, G., RIEDER, D., HACKL, H.,
597 KROGSDAM, A., LONCOVA, Z., POSCH, W., WILFLINGSEDER, D., SOPPER, S.,
598 IJSSELSTEIJN, M., BROUWER, T. P., JOHNSON, D., XU, Y., WANG, Y., SANDERS,
599 M. E., ESTRADA, M. V., ERICSSON-GONZALEZ, P., CHAROENTONG, P., BALKO, J.,
600 DE MIRANDA, N. & TRAJANOSKI, Z. 2019. Molecular and pharmacological modulators
601 of the tumor immune contexture revealed by deconvolution of RNA-seq data. *Genome*
602 *Med,* 11**,** 34.
603 GAUTAM, U. S., FOREMAN, T. W., BUCSAN, A. N., VEATCH, A. V., ALVAREZ, X.,
604 ADEKAMBI, T., GOLDEN, N. A., GENTRY, K. M., DOYLE-MEYERS, L. A., RUSSELL-
605 LODRIGUE, K. E., DIDIER, P. J., BLANCHARD, J. L., KOUSOULAS, K. G., LACKNER,
606 A. A., KALMAN, D., RENGARAJAN, J., KHADER, S. A., KAUSHAL, D. & MEHRA, S.

607 2018. In vivo inhibition of tryptophan catabolism reorganizes the tuberculoma and
608 augments immune-mediated control of Mycobacterium tuberculosis. *Proc Natl Acad Sci*
609 *U S A,* 115**,** E62-E71.
610 GAYNOR, C. D., MCCORMACK, F. X., VOELKER, D. R., MCGOWAN, S. E. &
611 SCHLESINGER, L. S. 1995. Pulmonary surfactant protein A mediates enhanced
612 phagocytosis of Mycobacterium tuberculosis by a direct interaction with human
613 macrophages. *J Immunol,* 155**,** 5343-51.
614 GUIRADO, E., SCHLESINGER, L. S. & KAPLAN, G. 2013. Macrophages in tuberculosis: Friend
615 or foe. *Semin. Immunopathol,* 35**,** 563-583.
616 HANDELMAN, S. K., SEWERYN, M., SMITH, R. M., HARTMANN, K., WANG, D., PIETRZAK,
617 M., JOHNSON, A. D., KLOCZKOWSKI, A. & SADEE, W. 2015. Conditional entropy in
618 variation-adjusted windows detects selection signatures associated with expression
619 quantitative trait loci (eQTLs). *BMC Genomics,* 16 Suppl 8**,** S8.
620 JOHNSON, W. E., LI, C. & RABINOVIC, A. 2007. Adjusting batch effects in microarray
621 expression data using empirical Bayes methods. *Biostatistics,* 8**,** 118-27.
622 LANGFELDER, P. & HORVATH, S. 2008. WGCNA: an R package for weighted correlation
623 network analysis. *BMC Bioinformatics,* 9**,** 559.
624 LAVALETT, L., RODRIGUEZ, H., ORTEGA, H., SADEE, W., SCHLESINGER, L. S. &
625 BARRERA, L. F. 2017. Alveolar macrophages from tuberculosis patients display an
626 altered inflammatory gene expression profile. *Tuberculosis (Edinb),* 107**,** 156-167.
627 LE, Y., CAO, W., ZHOU, L., FAN, X., LIU, Q., LIU, F., GAI, X., CHANG, C., XIONG, J., RAO, Y.,
628 LI, A., XU, W., LIU, B., WANG, T., WANG, B. & SUN, Y. 2020. Infection of
629 Mycobacterium tuberculosis Promotes Both M1/M2 Polarization and MMP Production in
630 Cigarette Smoke-Exposed Macrophages. *Front Immunol,* 11**,** 1902.
631 LEVENE, H. 1960. Robust tests for equality of variances. *In:* INGRAM OLKIN, H. H. E. A. (ed.)
632 *Contributions to Probability and Statistics.* Stanford University Press.

633 LI, P., HAO, Z., WU, J., MA, C., XU, Y., LI, J., LAN, R., ZHU, B., REN, P., FAN, D. & SUN, S.
634 2021. Comparative Proteomic Analysis of Polarized Human THP-1 and Mouse
635 RAW264.7 Macrophages. *Front Immunol,* 12**,** 700009.
636 LI, X., FU, Y., WANG, X., DEMEO, D. L., TANTISIRA, K., WEISS, S. T. & QIU, W. 2018.
637 Detecting Differentially Variable MicroRNAs via Model-Based Clustering. *Int J*
638 *Genomics,* 2018**,** 6591634.
639 LIAO, Y., WANG, J., JAEHNIG, E. J., SHI, Z. & ZHANG, B. 2019. WebGestalt 2019: gene set
640 analysis toolkit with revamped UIs and APIs. *Nucleic Acids Res,* 47**,** W199-W205.
641 LIU, C. H., LIU, H. & GE, B. 2017. Innate immunity in tuberculosis: host defense vs pathogen
642 evasion. *Cell Mol Immunol,* 14**,** 963-975.
643 LOVE, M. I., HUBER, W. & ANDERS, S. 2014. Moderated estimation of fold change and
644 dispersion for RNA-seq data with DESeq2. *Genome Biol,* 15**,** 550.
645 MOORES, R. C., BRILHA, S., SCHUTGENS, F., ELKINGTON, P. T. & FRIEDLAND, J. S. 2017.
646 Epigenetic Regulation of Matrix Metalloproteinase-1 and -3 Expression in
647 Mycobacterium tuberculosis Infection. *Front Immunol,* 8**,** 602.
648 MOREIRA-TEIXEIRA, L., TABONE, O., GRAHAM, C. M., SINGHANIA, A., STAVROPOULOS,
649 E., REDFORD, P. S., CHAKRAVARTY, P., PRIESTNALL, S. L., SUAREZ-BONNET, A.,
650 HERBERT, E., MAYER-BARBER, K. D., SHER, A., FONSECA, K. L., SOUSA, J., CA,
651 B., VERMA, R., HALDAR, P., SARAIVA, M. & O'GARRA, A. 2020. Mouse transcriptome
652 reveals potential signatures of protection and pathogenesis in human tuberculosis. *Nat*
653 *Immunol,* 21**,** 464-476.
654 MORTAZAVI, A., WILLIAMS, B. A., MCCUE, K., SCHAEFFER, L. & WOLD, B. 2008. Mapping
655 and quantifying mammalian transcriptomes by RNA-Seq. *Nat. Methods,* 5**,** 621-628.
656 NARANBHAI, V. 2016. The Role of Host Genetics (and Genomics) in Tuberculosis. *Microbiol*
657 *Spectr,* 4.

658 NGUYEN, H. A., RAJARAM, M. V., MEYER, D. A. & SCHLESINGER, L. S. 2012. Pulmonary
659 surfactant protein A and surfactant lipids upregulate IRAK-M, a negative regulator of
660 TLR-mediated inflammation in human macrophages. *Am J Physiol Lung Cell Mol*
661 *Physiol,* 303**,** L608-16.
662 ORECCHIONI, M., GHOSHEH, Y., PRAMOD, A. B. & LEY, K. 2019. Macrophage Polarization:
663 Different Gene Signatures in M1(LPS+) vs. Classically and M2(LPS-) vs. Alternatively
664 Activated Macrophages. *Front Immunol,* 10**,** 1084.
665 PAI, M., BEHR, M. A., DOWDY, D., DHEDA, K., DIVANGAHI, M., BOEHME, C. C.,
666 GINSBERG, A., SWAMINATHAN, S., SPIGELMAN, M., GETAHUN, H., MENZIES, D. &
667 RAVIGLIONE, M. 2016. Tuberculosis. *Nat Rev Dis Primers,* 2**,** 16076.
668 PAPP, A. C., AZAD, A. K., PIETRZAK, M., WILLIAMS, A., HANDELMAN, S. K., IGO, R. P., JR.,
669 STEIN, C. M., HARTMANN, K., SCHLESINGER, L. S. & SADEE, W. 2018. AmpliSeq
670 transcriptome analysis of human alveolar and monocyte-derived macrophages over time
671 in response to Mycobacterium tuberculosis infection. *PLoS One,* 13**,** e0198221.
672 RAJARAM, M. V., NI, B., DODD, C. E. & SCHLESINGER, L. S. 2014. Macrophage
673 immunoregulatory pathways in tuberculosis. *Semin. Immunol,* 26**,** 471-485.
674 RAJARAM, M. V., NI, B., MORRIS, J. D., BROOKS, M. N., CARLSON, T. K.,
675 BAKTHAVACHALU, B., SCHOENBERG, D. R., TORRELLES, J. B. & SCHLESINGER,
676 L. S. 2011. *Mycobacterium tuberculosis* lipomannan blocks TNF biosynthesis by
677 regulating macrophage MAPK-activated protein kinase 2 (MK2) and microRNA miR-
678 125b. *Proc Natl Acad Sci U S A,* 108**,** 17408-13.
679 REFAI, A., GRITLI, S., BARBOUCHE, M. R. & ESSAFI, M. 2018. Mycobacterium tuberculosis
680 Virulent Factor ESAT-6 Drives Macrophage Differentiation Toward the Pro-inflammatory
681 M1 Phenotype and Subsequently Switches It to the Anti-inflammatory M2 Phenotype.
682 *Front Cell Infect Microbiol,* 8**,** 327.

683 ROTHCHILD, A. C., OLSON, G. S., NEMETH, J., AMON, L. M., MAI, D., GOLD, E. S.,
684 DIERCKS, A. H. & ADEREM, A. 2019. Alveolar macrophages generate a noncanonical
685 NRF2-driven transcriptional response to Mycobacterium tuberculosis in vivo. *Sci*
686 *Immunol,* 4.
687 ROY, S., SCHMEIER, S., KACZKOWSKI, B., ARNER, E., ALAM, T., OZTURK, M., TAMGUE,
688 O., PARIHAR, S. P., KAWAJI, H., ITOH, M., LASSMANN, T., CARNINCI, P.,
689 HAYASHIZAKI, Y., FORREST, A. R. R., GULER, R., BAJIC, V. B., BROMBACHER, F.
690 & SUZUKI, H. 2018. Transcriptional landscape of Mycobacterium tuberculosis infection
691 in macrophages. *Sci Rep,* 8**,** 6758.
692 SALUNKE, S. B., AZAD, A. K., KAPURIYA, N. P., BALADA-LLASAT, J. M., PANCHOLI, P.,
693 SCHLESINGER, L. S. & CHEN, C. S. 2015. Design and synthesis of novel anti-
694 tuberculosis agents from the celecoxib pharmacophore. *Bioorg Med Chem,* 23**,** 1935-43.
695 SCHLESINGER, L. S., BELLINGERKAWAHARA, C. G., PAYNE, N. R. & HORWITZ, M. A.
696 1990. Phagocytosis of Mycobacterium-Tuberculosis Is Mediated by Human Monocyte
697 Complement Receptors and Complement Component-C3. *Journal of Immunology,* 144**,**
698 2771-2780.
699 SCHOREY, J. S. & SCHLESINGER, L. S. 2016. Innate Immune Responses to Tuberculosis.
700 *Microbiol Spectr,* 4.
701 SOUSA, J., CA, B., MACEIRAS, A. R., SIMOES-COSTA, L., FONSECA, K. L., FERNANDES,
702 A. I., RAMOS, A., CARVALHO, T., BARROS, L., MAGALHAES, C., CHINER-OMS, A.,
703 MACHADO, H., VEIGA, M. I., SINGH, A., PEREIRA, R., AMORIM, A., VIEIRA, J.,
704 VIEIRA, C. P., BHATT, A., RODRIGUES, F., RODRIGUES, P. N. S., GAGNEUX, S.,
705 CASTRO, A. G., GUIMARAES, J. T., BASTOS, H. N., OSORIO, N. S., COMAS, I. &
706 SARAIVA, M. 2020. Mycobacterium tuberculosis associated with severe tuberculosis
707 evades cytosolic surveillance systems and modulates IL-1beta production. *Nat*
708 *Commun,* 11**,** 1949.

709 TAMERIS, M. D., HATHERILL, M., LANDRY, B. S., SCRIBA, T. J., SNOWDEN, M. A.,
710 LOCKHART, S., SHEA, J. E., MCCLAIN, J. B., HUSSEY, G. D., HANEKOM, W. A.,
711 MAHOMED, H. & MCSHANE, H. 2013. Safety and efficacy of MVA85A, a new
712 tuberculosis vaccine, in infants previously vaccinated with BCG: a randomised, placebo-
713 controlled phase 2b trial. *Lancet,* 381**,** 1021-1028.
714 THUONG, N. T., DUNSTAN, S. J., CHAU, T. T., THORSSON, V., SIMMONS, C. P., QUYEN, N.
715 T., THWAITES, G. E., THI NGOC, L. N., HIBBERD, M., TEO, Y. Y., SEIELSTAD, M.,
716 ADEREM, A., FARRAR, J. J. & HAWN, T. R. 2008. Identification of tuberculosis
717 susceptibility genes with human macrophage gene expression profiles. *PLoS. Pathog,* 4**,**
718 e1000229.
719 UREN, C., HENN, B. M., FRANKE, A., WITTIG, M., VAN HELDEN, P. D., HOAL, E. G. &
720 MOLLER, M. 2017. A post-GWAS analysis of predicted regulatory variants and
721 tuberculosis susceptibility. *PLoS One,* 12**,** e0174738.
722 VIOLA, A., MUNARI, F., SANCHEZ-RODRIGUEZ, R., SCOLARO, T. & CASTEGNA, A. 2019.
723 The Metabolic Signature of Macrophage Responses. *Front Immunol,* 10**,** 1462.
724 WHO 2020. Global tuberculosis report 2020. Geneva: World Health Organization.
725 WU, K., FANG, H., LYU, L. D., LOWRIE, D. B., WONG, K. W. & FAN, X. Y. 2014. A derived
726 network-based interferon-related signature of human macrophages responding to
727 Mycobacterium tuberculosis. *Biomed Res Int,* 2014**,** 713071.
728 XUE, J., SCHMIDT, S. V., SANDER, J., DRAFFEHN, A., KREBS, W., QUESTER, I., DE
729 NARDO, D., GOHEL, T. D., EMDE, M., SCHMIDLEITHNER, L., GANESAN, H., NINO-
730 CASTRO, A., MALLMANN, M. R., LABZIN, L., THEIS, H., KRAUT, M., BEYER, M.,
731 LATZ, E., FREEMAN, T. C., ULAS, T. & SCHULTZE, J. L. 2014. Transcriptome-based
732 network analysis reveals a spectrum model of human macrophage activation. *Immunity,*
733 40**,** 274-88.

734 XUE, Z. T., SJOGREN, H. O., SALFORD, L. G. & WIDEGREN, B. 2012. An epigenetic
735 mechanism for high, synergistic expression of indoleamine 2,3-dioxygenase 1 (IDO1) by
736 combined treatment with zebularine and IFN-gamma: potential therapeutic use in
737 autoimmune diseases. *Mol Immunol,* 51**,** 101-11.
738 ZAK, D. E., PENN-NICHOLSON, A., SCRIBA, T. J., THOMPSON, E., SULIMAN, S., AMON, L.
739 M., MAHOMED, H., ERASMUS, M., WHATNEY, W., HUSSEY, G. D., ABRAHAMS, D.,
740 KAFAAR, F., HAWKRIDGE, T., VERVER, S., HUGHES, E. J., OTA, M., SUTHERLAND,
741 J., HOWE, R., DOCKRELL, H. M., BOOM, W. H., THIEL, B., OTTENHOFF, T. H. M.,
742 MAYANJA-KIZZA, H., CRAMPIN, A. C., DOWNING, K., HATHERILL, M., VALVO, J.,
743 SHANKAR, S., PARIDA, S. K., KAUFMANN, S. H. E., WALZL, G., ADEREM, A.,
744 HANEKOM, W. A., ACS & GROUPS, G. C. C. S. 2016. A blood RNA signature for
745 tuberculosis disease risk: a prospective cohort study. *Lancet,* 387**,** 2312-2322.

746

Figure 1 - figure supplement 1. **The transcriptional response of 28 human AM cultures to *in vitro* incubation and to *M.tb* infection.** A principle component analysis of normalized gene expression reveals the impact of cell culture conditions with and without *M.tb* infection.

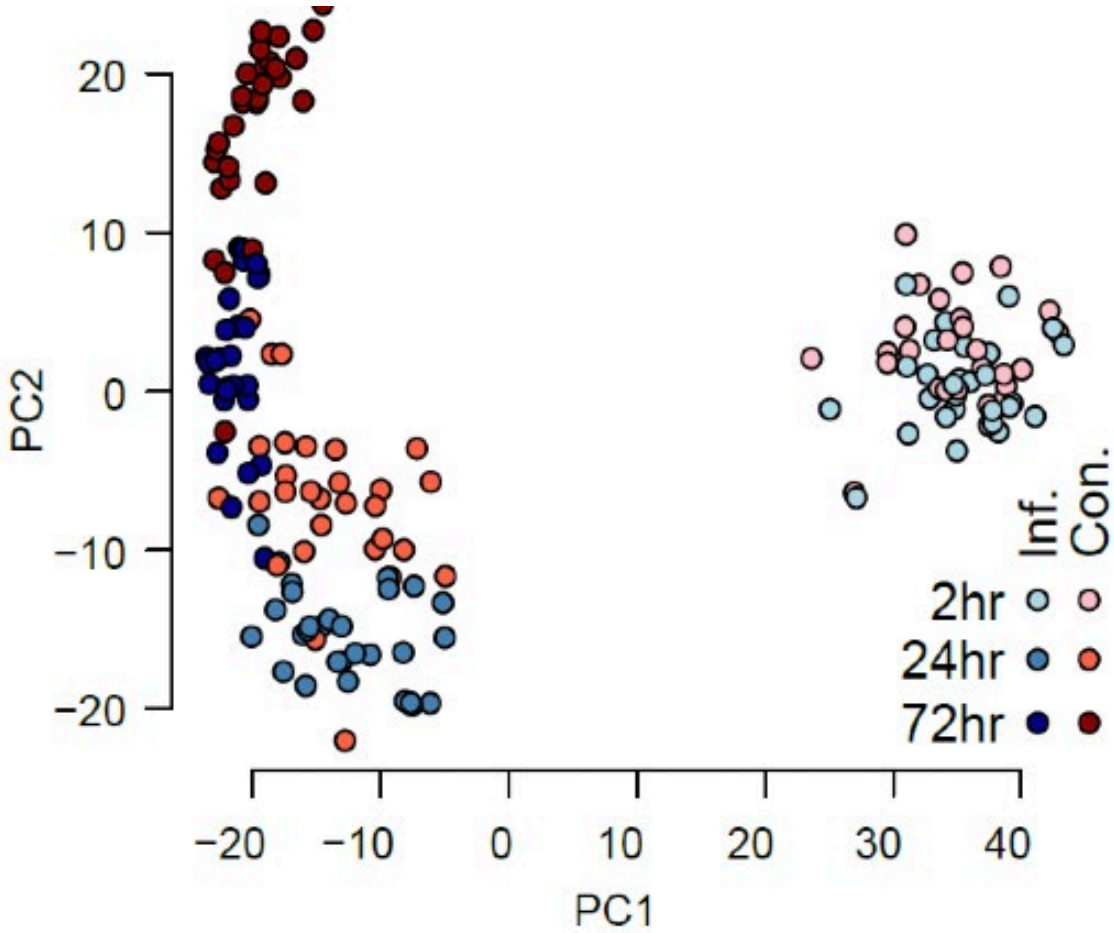
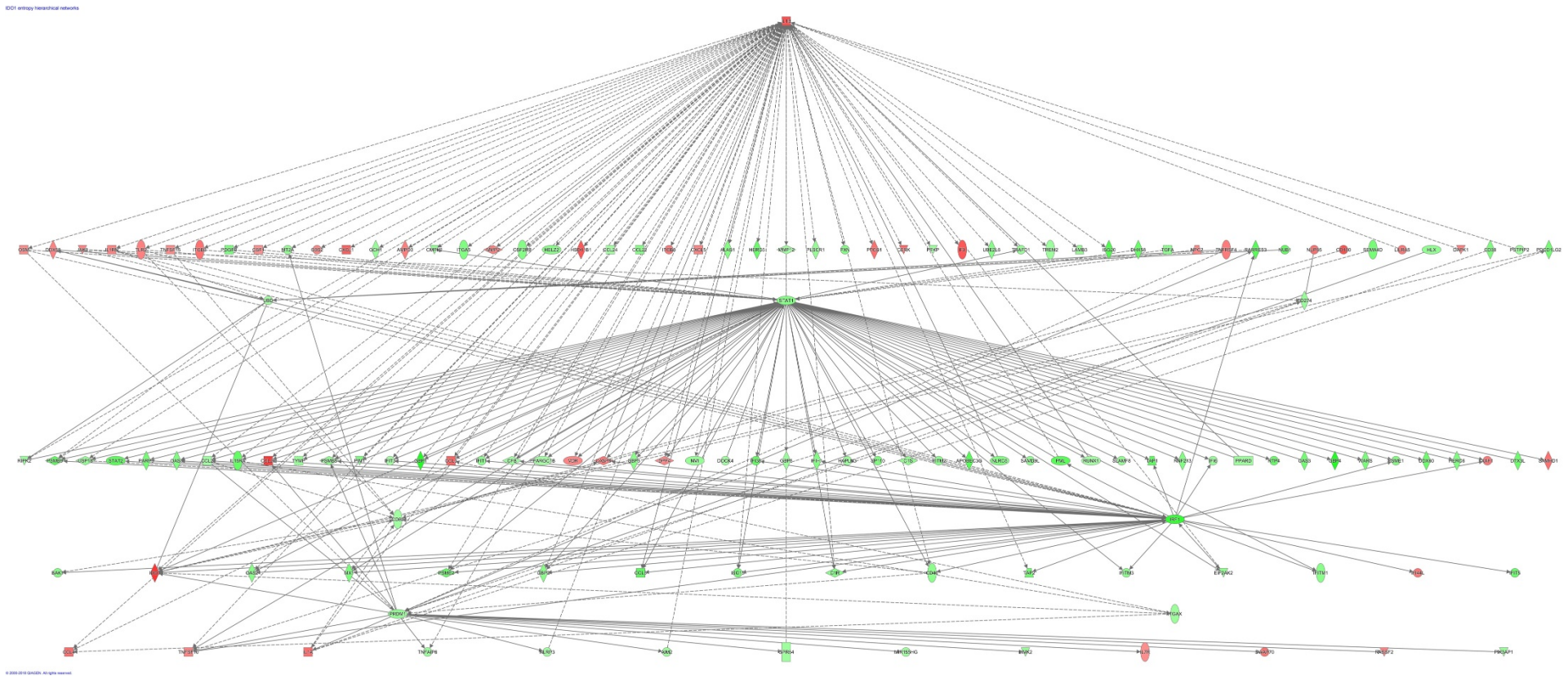
Figure 7 – figure supplement 1. Top scoring network of DE genes with highly variable expression (VE/DE genes). The Ingenuity Pathway Analysis (IPA) (https://www.qiagenbioinformatics.com/products/ingenuity-pathway-analysis/) of VE/DE genes (n=324) generates a top scoring gene network, with IL1B on top. The same pathway is shown in Figure 7, while this graph displays all gene names.